Actively coupled optical waveguides

N. V. Alexeeva,[1,2] I. V. Barashenkov,[1,2] K. Rayanov,[1] and S. Flach[1]

[1]*New Zealand Institute for Advanced Study, Centre for Theoretical Chemistry and Physics, Massey University, Auckland 0745, New Zealand*

[2]*Department of Mathematics and Centre for Theoretical and Mathematical Physics, University of Cape Town, Rondebosch 7701, South Africa*

(Received 26 May 2013; published 30 January 2014)

We consider light propagation through a pair of nonlinear optical waveguides with absorption, placed in a medium with power gain. The active medium boosts the in-phase component of the overlapping evanescent fields of the guides, while the nonlinearity of the guides couples it to the damped out-of-phase component creating a feedback loop. As a result, the structure exhibits stable stationary and oscillatory regimes in a wide range of gain-loss ratios. We show that the pair of actively coupled ($\mathcal{AC}$) waveguides can act as a stationary or integrate-and-fire comparator sensitive to tiny differences in their input powers.

DOI: 10.1103/PhysRevA.89.013848 PACS number(s): 42.65.Wi, 42.82.Et, 42.65.Sf

I. INTRODUCTION

Nonlinear directional couplers are important for various applications in integrated optics, such as power-sensitive switches and polarization beam splitters. The twin core coupler is based on the coherent light exchange between two optical waveguides placed in close proximity. For low input intensities, the full power oscillates periodically between the two waveguides; for higher input levels, the total power is self-trapped mainly in one of the two channels [1].

The performance of the device can be improved—the switching power can be reduced while the length is shortened—by utilizing material losses. The effect of absorption which is usually regarded as an unavoidable hinderance, is therefore turned into an advantage here. The dissipation is balanced by introducing gain into one of the waveguides [2]. Thus, a nonlinear coupler composed of one core with a certain amount of gain and another one with an equal amount of loss switches the entire power to one waveguide [3]. Recently this type of a coupler has attracted a lot of attention as an experimental realization of a $\mathcal{PT}$-symmetric system [4]. It is worth noting here that the operation of the $\mathcal{PT}$-symmetric coupler requires the fine-tuning of gain and loss to secure their exact compensation. We also note that the power switching is accompanied by the unbounded power growth in one of the arms of the device—the growth not saturable by nonlinearity [4].

In this article, we propose an alternative configuration of gain and loss in the directional coupler. The arrangement consists of two lossy waveguides placed in an active medium. Instead of providing power gain in the core of a waveguide, the structure boosts the evanescent fields which couple the two channels due to their close proximity. With the choice of the symmetric gain configuration, the energy is pumped into the in-phase linear mode of the two-waveguide system while the antiphase normal mode remains lossy.

The operation of the outlined device (the actively coupled pair of waveguides, or simply the "$\mathcal{AC}$ coupler") is conditional on the presence of nonlinearity. As the symmetric mode starts to grow, it activates the nonlinear response in each waveguide. The nonlinearity couples the symmetric mode to the antisymmetric mode, and the latter drains the energy out of the system securing the overall power balance. The concept admits generalizations to networks of waveguides, with various coupling geometries.

The principle of active coupling is not confined to the realm of nonlinear optics. It can be utilized in any physical setting consisting of two identical lossy elements, where the energy is pumped into the symmetric normal mode of the coupled system. One example of such a dimer is the atomic Bose-Einstein condensate in a double-well trapping potential [5] with finite external barriers (allowing the leakage of atoms out of the system [6]) and the particle injection in the interwell region. (See Ref. [7] for the quantum version.) Other examples include coupled LRC (resistor-inductor-capacitor) circuits [8] and structured metamaterials consisting of pairs of nonlinear split-ring resonators [9]. A similar principle underlies the radiative coupling and weak lasing of exciton-polariton condensates [10]. The latter are highly dissipative coherent condensates of quasiparticles, where the finiteness of the quasiparticle lifetime is compensated by an external pump.

The $\mathcal{AC}$ coupler is structurally stable; in order to ensure the gain-loss balance, one need not strive to secure the perfect equality of gain and loss. Instead, the loss compensation is achieved in a finite band of gain coefficients. Unlike the usual nonlinear optical coupler, and unlike the $\mathcal{PT}$ coupler, the observable regimes in the new configuration are determined by the system parameter values rather than initial conditions. Furthermore, the system does not exhibit any uncontrollable growth of optical modes.

II. MODEL

In a single-mode optical waveguide, the optical field is described by a complex amplitude, $\Psi(x,y,z) = E(x,y)\psi(z)$, where (x,y) is the plane transversal to the waveguide axis z. The eigenfunction $E(x,y)$ decays away from the waveguide core and can be chosen to be real and everywhere positive, with the norm $\int E^2 dxdy = 1$.

We consider two parallel identical waveguides. Denoting x as the coordinate in the direction connecting their centers, we choose the origin halfway between them. The individual eigenfunctions E_1 and E_2 are then centered at $x = -x_0$ and $x = x_0$, respectively, and satisfy $E_1(x,y) = E_2(-x,y)$. The waveguides are embedded in the active medium (Fig. 1) and gain power through the response of the medium to the evanescent part of their fields, Ψ_1 and Ψ_2.

The integral gain of the amplitude $\psi_n(z)$ over the entire active region is $\int \alpha E_n(x,y)\Psi dxdy$, where $\Psi(x,y,z)$ is the sum

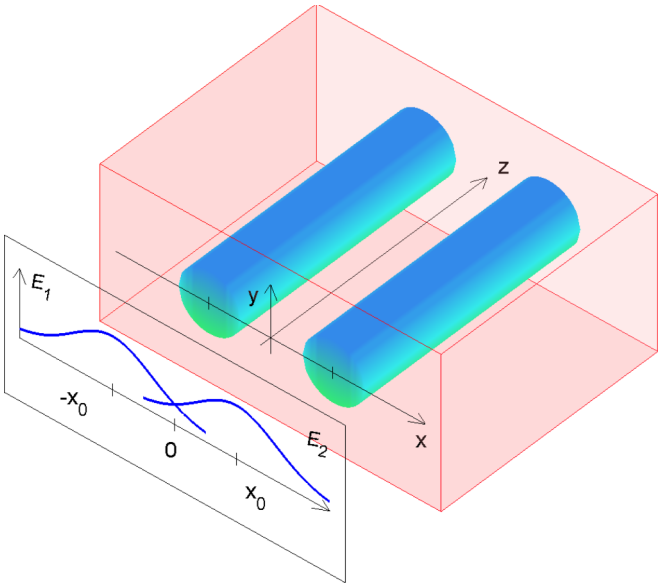

FIG. 1. (Color online) The $\mathcal{AC}$ coupler: two parallel lossy waveguides coupled via an active medium. The stand-alone vertical plane shows the eigenfunctions $E_1(x,0)$ and $E_2(x,0)$.

of the two evanescent fields: $\Psi = \Psi_1(x,y,z) + \Psi_2(x,y,z)$. The coefficient $\alpha(x,y) \geqslant 0$ characterizes the active properties of the medium. The integral gain in the n-th waveguide is then $a_{n1}\psi_1 + a_{n2}\psi_2$, where

$$a_{nm} = \int \alpha(x,y)E_n(x,y)E_m(x,y)dxdy, \quad n,m = 1,2.$$

With the gain added, the amplitudes ψ_1 and ψ_2 satisfy

$$\frac{d\psi_1}{dz} + \Gamma\psi_1 = i\mathcal{T}\psi_2 + i\beta|\psi_1|^2\psi_1 + \sum a_{1n}\psi_n, \quad (1a)$$

$$\frac{d\psi_2}{dz} + \Gamma\psi_2 = i\mathcal{T}\psi_1 + i\beta|\psi_2|^2\psi_2 + \sum a_{2n}\psi_n. \quad (1b)$$

Here Γ is the loss rate, β is the nonlinearity strength, and $\mathcal{T}$ quantifies light tunneling between the guides [11]. In what follows, we assume the focusing nonlinearity, $\beta > 0$. We scale $\psi_{1,2}$ so that $\beta = 1$ and we normalize $\mathcal{T}$ to 1.

We note that $a_{12} = a_{21}$. Assuming symmetric density distributions $\alpha(x,y) = \alpha(-x,y)$ we also have $a_{11} = a_{22}$. From $E_{1,2}(x,y) > 0$ it follows that $a_{mn} > 0$. Using the Schwartz inequality, one readily checks that a_{11} is always greater than a_{12}. All coefficients become equal only when the active region is very thin: $\alpha(x,y) = \alpha_0(y)\delta(x)$. In this case we have $a_{11} = a_{12} = \int \alpha_0(y)E_1^2(0,y)dy$.

In the general situation of symmetrically distributed gain, we introduce the net loss rate $\gamma = \Gamma - a_{11}$ and the active coupling ($\mathcal{AC}$) coefficient $a \equiv a_{12}$ to obtain

$$\frac{d\psi_1}{dz} + \gamma\psi_1 = i\psi_2 + i|\psi_1|^2\psi_1 + a\psi_2, \quad (2a)$$

$$\frac{d\psi_2}{dz} + \gamma\psi_2 = i\psi_1 + i|\psi_2|^2\psi_2 + a\psi_1. \quad (2b)$$

In this article, we consider the regime where $\gamma > 0$.

III. DYNAMICS OF COUPLED BEAMS

When the net loss exceeds the $\mathcal{AC}$ gain ($\gamma > a$), all solutions of Eq. (2) decay to zero:

$$\frac{dP}{dz} \leqslant 2(a-\gamma)P. \quad (3)$$

Here $P = |\psi_1|^2 + |\psi_2|^2$ is the total power of light in the coupler. Thus in the region below the $\gamma = a$ line in Fig. 2, the origin $\psi_1 = \psi_2 = 0$ is a globally stable fixed point.

Introducing the symmetric and antisymmetric normal modes $u = \psi_1 + \psi_2$ and $v = \psi_1 - \psi_2$ diagonalizes the linear part of Eq. (2)—but couples the nonlinear terms:

$$\frac{du}{dz} + (\gamma - a - i)u = \frac{i}{4}[(|u|^2 + 2|v|^2)u + v^2u^*], \quad (4a)$$

$$\frac{dv}{dz} + (\gamma + a + i)v = \frac{i}{4}[(2|u|^2 + |v|^2)v + u^2v^*]. \quad (4b)$$

According to Eq. (4a), making a greater than γ turns the origin into an unstable fixed point. In the $a > \gamma$ regime with $v(0) = 0$, the symmetric mode grows without bound. However the blow-up of the u mode can be arrested by its nonlinear coupling to the antisymmetric mode.

Decomposing the complex amplitudes as $\psi_1 = \sqrt{P_1}e^{i\phi}$ and $\psi_2 = \sqrt{P_2}e^{i(\phi+\theta)}$, we observe that the common part of the phases of the two beams is expressible through the powers

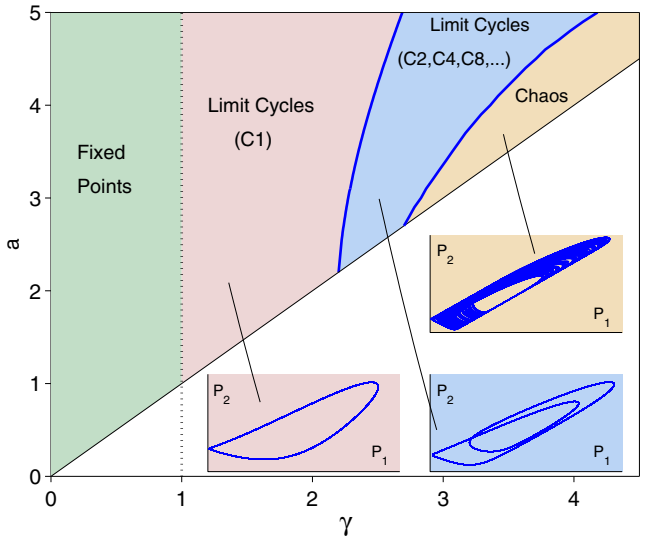

FIG. 2. (Color online) The chart of attractors on the (γ,a) plane. In the empty area below the $\gamma = a$ line, all initial conditions decay to zero as $t \to \infty$. In the green strip, the attractors are the fixed points $F^{\pm}$. Pink marks the region where all trajectories wind onto one of the two limit cycles $C^{\pm}$, with one simple oscillation per period (hence "C1"). In the blue domain the attracting cycles have 2^n (i.e., 2,4,8, ...) simple oscillations per period. Ochre colors the area where the attractors are predominantly chaotic; these consist of repeated oscillations with randomly selected amplitudes. Three insets are phase portraits on the (P_1,P_2) plane: a cycle with one and two oscillations per period and a chaotic attractor.

they carry and their phase difference:

$$\phi(z) = \int_0^z \left[P_1 + \sqrt{\frac{P_2}{P_1}}(\cos\theta + a\sin\theta) \right] dz + \phi(0).$$

Therefore out of four real variables in the system (2) only three represent independent degrees of freedom.

This fact is made obvious by transforming the system to an explicitly three-dimensional form:

$$\dot{X} = -\gamma X - Y, \tag{5a}$$

$$\dot{Y} = -\gamma Y + X - XZ, \tag{5b}$$

$$\dot{Z} = -\gamma Z + ar + XY. \tag{5c}$$

Here $X = \frac{1}{2}(|\psi_1|^2 - |\psi_2|^2)$ measures the power imbalance between the two waveguides; $Y = \frac{i}{2}(\psi_1\psi_2^* - \psi_1^*\psi_2)$ characterizes the energy flux from the first to the second channel, and $2aZ$—where $Z = \frac{1}{2}(\psi_1\psi_2^* + \psi_2\psi_1^*)$—is the total gain in the system. The Stokes variables X, Y, and Z are three components of the vector $\mathbf{r}$, with $r = \sqrt{\mathbf{r}^2} = P/2$. The overdot indicates differentiation with respect to the fictitious time variable, $t = 2z$, which we introduce for the convenience of analysis.

The beam powers $P_{1,2}$ and the phase difference θ can be easily reconstructed from the Stokes variables: $P_{1,2} = r \pm X$ and $\tan\theta = Y/Z$. We also note a similarity between Eqs. (5) and the Lorentz system [12].

IV. SYMMETRY-BROKEN FIXED POINTS

Like the Lorentz system, Eqs. (5) are symmetric under the reflection of X and Y. As the $\mathcal{AC}$ coefficient is increased beyond $a = \gamma$ in the weakly dissipative regime ($\gamma < 1$), the fixed point at the origin suffers a symmetry-breaking (pitchfork) bifurcation. Two stable fixed points F^+ and F^- are born, supercritically. These points share the values of r and Z,

$$r = (\gamma^2 + 1)\frac{a}{\gamma}, \quad Z = \frac{\gamma}{a}r, \tag{6}$$

but have opposite X and Y,

$$X = -\frac{\sigma}{a}r, \quad Y = \sigma\frac{\gamma}{a}r. \tag{7}$$

The point F^+ has $\sigma > 0$ and F^- has $\sigma < 0$, where $\sigma^2 = (a^2 - \gamma^2)/(\gamma^2 + 1)$. The two points are therefore mirror images of each other.

Either of the two fixed points represents a pair of light beams with constant, z-independent, power in each channel. The point F^+ corresponds to a greater power in the second channel ($P_1/P_2 \approx \gamma^2/2$ for small γ), while its mirror reflection F^- has the inverse power ratio. The phases ϕ_1 and ϕ_2 pertaining to the points $F^\pm$ are linear functions of z, with the phase difference θ remaining constant.

Figure 3(a) depicts the evolution of the input with a small power imbalance. We observe that taking $P_2(0)$ only slightly greater than $P_1(0)$ is sufficient to select the stationary regime (F^+) with $P_2 \gg P_1$.

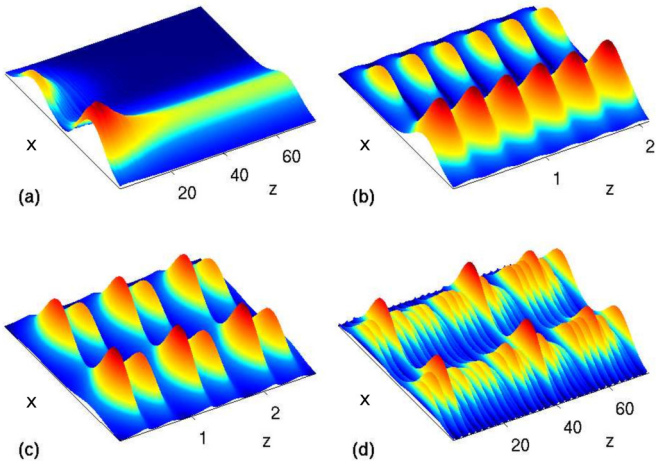

FIG. 3. (Color online) Characteristic regimes of the $\mathcal{AC}$ coupler. Shown is $|E_1(x,0)\psi_1(z) + E_2(x,0)\psi_2(z)|^2$, with the eigenfunctions exemplified by $E_{1,2}(x,0) = \frac{1}{\sqrt{2\pi}\nu}\exp(\frac{-(x\pm x_0)^2}{2\nu^2})$, $\nu = \frac{3}{5}x_0$. (a) The stationary regime F^+ evolving out of the initial condition with $P_1 = 30$, $P_2 = 33$, and $\theta = 0$. Here $a = 1$ and $\gamma = 0.1$. (b) The limit cycle C^+ ($a = 9$, $\gamma = 1.5$). (c) The limit cycle with two oscillations per period ($a = 9$, $\gamma = 4.2$). (d) The chaotic attractor ($a = 9$, $\gamma = 7.6$).

V. PERIODIC AND CHAOTIC REGIMES

Linearizing Eqs. (5) about either of the fixed points $F^\pm$ yields the Jacobian matrix with one real negative and two complex-conjugate eigenvalues λ. Assume the active coupling is fixed above the threshold value $a = 1$ and the net loss γ is varied. As γ is increased through $\gamma_c = 1$, the complex eigenvalues cross from $\mathrm{Re}\,\lambda < 0$ to $\mathrm{Re}\,\lambda > 0$. This is the signature of the Hopf bifurcation where both F^+ and F^- lose their stability while two stable limit cycles of small radius are born—one around each fixed point.

The limit cycles describe periodic variation of the powers $P_{1,2}$ carried by the two waveguides [Fig. 3(b)]. We denote the cycle born around the point F^+ as C^+ and the cycle bifurcating from F^- as C^-.

Like their parent fixed points $F^\pm$, the limit cycles $C^\pm$ are symmetry broken. The cycle C^+ has the second waveguide carrying higher power than the first one, while its mirror-reflected counterpart C^- has $P_1(z) > P_2(z)$ for all z. When

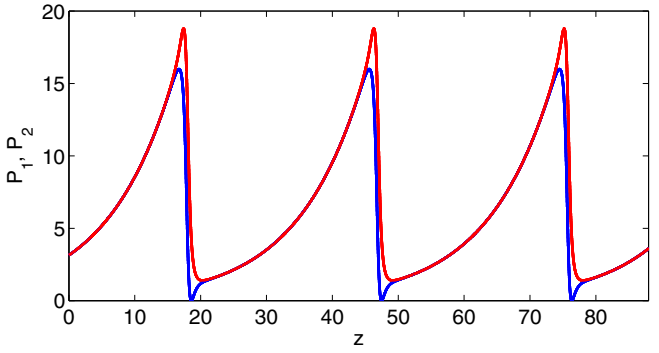

FIG. 4. (Color online) The integrate-and-fire limit cycle arising for γ close to a. (In this plot, $\gamma = 1.9$ and $a = 2$.) The red and blue line show P_2 and P_1, respectively.

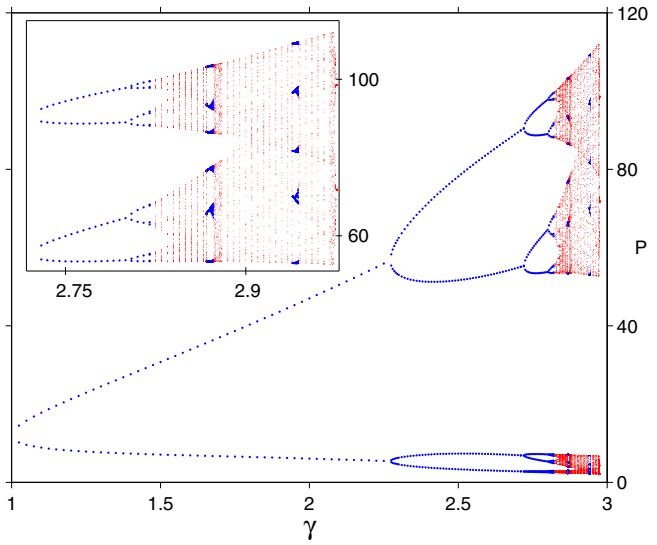

FIG. 5. (Color online) The period-doubling transition to chaos for $a = 3$. The local minima and maxima of the function $P(z)$ are plotted against the corresponding value of the loss coefficient. The inset shows a fine structure of the chaotic region. Periodic orbits are highlighted (colored blue in the online version), while chaotic attractors are marked by lighter points (red online).

$\gamma = \gamma_c$, the frequency of each cycle is given by $\omega = \mathrm{Im}\,\lambda = \sqrt{a^2 - 1}$. As γ is increased beyond γ_c, the radius of each cycle grows and the frequency changes.

The limit cycles with γ near a display an integrate-and-fire switch dynamics (Fig. 4). Namely, the powers in the two waveguides grow slowly and synchronously, with one of these (say, P_1) remaining only slightly smaller than the other power (P_2). This is followed by a quick discharge, where the first waveguide loses practically all its power ($P_1 = 0$) while P_2 remains nonzero.

As the loss γ is increased with the value of active coupling fixed above $a = 2.2$, the limit cycle suffers a period doubling. The emerging periodic attractor with two oscillations per period is shown in Fig. 3(c) and the middle inset in Fig. 2. When γ is increased further, the limit cycle undergoes a cascade of higher period-doubling bifurcations (Fig. 5). This culminates in the emergence of chaotic attractors [Fig. 3(d) and the top inset in Fig. 2]. The set of parameter values corresponding to periodic attractors with 2^n oscillations per period ($n = 1,2,\ldots$) is shown in blue in Fig. 2, and the "chaotic domain" is ochre colored.

VI. CONCLUSIONS

We conclude our study of the $\mathcal{AC}$ coupler by crystallizing its key difference from the $\mathcal{PT}$-symmetric device. While the latter balances gain in one waveguide with loss in the other, the former treats its two channels equally. It is the symmetric and antisymmetric normal modes (rather than the two guides themselves) that serve as the gain and loss agents in the $\mathcal{AC}$ configuration.

An important advantage of the $\mathcal{AC}$ coupler is its structural stability. For the given loss rate, the system supports stationary and periodic light beams in a wide range of gain coefficients rather than for a particular value of a. This is a fundamental distinction from the $\mathcal{PT}$-symmetric coupler where one has to tune the gain to match the loss exactly [4].

The new properties exhibited by the device can be utilized in a variety of applications. One possible setting is an optical analog of the voltage comparator which swings its output to one of two values depending on the relation between its two input voltages. The $\mathcal{AC}$ coupler can operate either in the stationary regime, where the two output values are given by the fixed points of the system (5), or as an integrate-and-fire switch (Fig. 4), where one of the waveguides is left powerless periodically. The period of this oscillator can be tuned simply by varying the distance between the waveguides. Unlike the $\mathcal{PT}$-symmetric coupler, no input can trigger an uncontrollable growth of optical modes in the $\mathcal{AC}$ switch.

Finally, we note that the left-right symmetry in the arrangement of two elements is not a prerequisite for their active coupling and the device operation. The stable light propagation requires only the presence of two linear modes, an excitable and a damped one, and the availability of their nonlinear coupling giving rise to a negative feedback loop. Even if the left-right symmetry of the structure is broken by small perturbations, the $\mathcal{AC}$ coupler will remain stably operational.

The principle of the $\mathcal{AC}$ coupling is therefore not exclusive to a pair of parallel waveguides but can be applied to a broad range of geometric designs. In particular, it would be interesting to consider the active coupling of two orthogonally polarized HE_{11} modes [13] of a single-mode fiber with gain in its cladding. On the other hand, the active coupling of spatial channels in a multicore fiber can improve characteristics of spatial-division multiplexing [14]. One more potential application of the $\mathcal{AC}$ coupling is to the blow-up-aided pulse compression in nonlinear fiber arrays [15].

ACKNOWLEDGMENTS

N.A.'s and I.B.'s sabbatical leave in Auckland was funded via visiting fellowships of the New Zealand Institute for Advanced Study. The project was also supported by the NRF of South Africa (Grants No. 85751 and No. 78950) and the Vera Davie Study and Research Bursary of the UCT.

[1] S. M. Jensen, IEEE J. Quantum Electron. **18**, 1580 (1982); A. W. Snyder and Y. Chen, Opt. Lett. **14**, 517 (1989).

[2] M. Premaratne and G. P. Agrawal, *Light Propagation in Gain Media* (Cambridge University Press, Cambridge, UK, 2011).

[3] Y. Chen, A. W. Snyder, and D. N. Payne, IEEE J. Quantum Electron. **28**, 239 (1992).

[4] H. Ramezani, T. Kottos, R. El-Ganainy, and D. N. Christodoulides, Phys. Rev. A **82**, 043803 (2010); A. A.

Sukhorukov, Z. Y. Xu, and Yu. S. Kivshar, *ibid.* **82**, 043818 (2010); C. E. Rüter, K. G. Makris, R. El-Ganainy, D. N. Christodoulides, M. Segev, and D. Kip, Nat. Phys. **6**, 192 (2010); T. Kottos, *ibid.* **6**, 166 (2010); Z. Lin, H. Ramezani, T. Eichelkraut, T. Kottos, H. Cao, and D. N. Christodoulides, Phys. Rev. Lett. **106**, 213901 (2011); A. Regensburger, C. Bersch, M.-A. Miri, G. Onishchukov, D. N. Christodoulides, and U. Peschel, Nature (London) **488**, 167 (2012).

[5] The Gross-Pitaevski equation for the condensate in the double-well potential admits two-mode approximations similar to the optical waveguide equations (1); see, e.g., S. Raghavan, A. Smerzi, S. Fantoni, and S. R. Shenoy, Phys. Rev. A **59**, 620 (1999); E. A. Ostrovskaya, Y. S. Kivshar, M. Lisak, B. Hall, F. Cattani, and D. Anderson, *ibid.* **61**, 031601(R) (2000); D. Ananikian and T. Bergeman, *ibid.* **73**, 013604 (2006); G. Theocharis, P. G. Kevrekidis, D. J. Frantzeskakis, and P. Schmelcher, Phys. Rev. E **74**, 056608 (2006).

[6] H. Cartarius and G. Wunner, Phys. Rev. A **86**, 013612 (2012); H. Cartarius, D. Haag, D. Dast, and G. Wunner, J. Phys. A: Math. Theor. **45**, 444008 (2012); E. M. Graefe, *ibid.* **45**, 444015 (2012); D. Dast, D. Haag, H. Cartarius, G. Wunner, R. Eichler, and J. Main, *ibid.* **61**, 124 (2013).

[7] M. Hiller, T. Kottos, and A. Ossipov, Phys. Rev. A **73**, 063625 (2006); E. M. Graefe, H. J. Korsch, and A. E. Niederle, Phys. Rev. Lett. **101**, 150408 (2008); Phys. Rev. A **82**, 013629 (2010).

[8] J. Schindler, A. Li, M. C. Zheng, F. M. Ellis, and T. Kottos, Phys. Rev. A **84**, 040101(R) (2011); J. Schindler, Z. Lin, J. M. Lee, H. Ramezani, F. M. Ellis, and T. Kottos, J. Phys. A: Math. Theor. **45**, 444029 (2012).

[9] N. Lazarides and G. P. Tsironis, Phys. Rev. Lett. **110**, 053901 (2013).

[10] I. L. Aleiner, B. L. Altshuler, and Y. G. Rubo, Phys. Rev. B **85**, 121301(R) (2012).

[11] A. W. Snyder and J. D. Love, *Optical Waveguide Theory* (Chapman & Hall, London, 1983).

[12] C. Sparrow, *The Lorenz Equations: Bifurcations, Chaos, and Strange Attractors*, Applied Mathematical Sciences Vol. 41 (Springer, New York, 1982).

[13] A. W. Snyder and R. A. Sammut, J. Opt. Soc. Am. **69**, 1663 (1979).

[14] S. K. Turitsyn, A. M. Rubenchik, M. P. Fedoruk, and E. Tkachenko, Phys. Rev. A **86**, 031804(R) (2012); A. M. Rubenchik, E. V. Tkachenko, M. P. Fedoruk, and S. K. Turitsyn, Opt. Lett. **38**, 4232 (2013).

[15] A. B. Aceves, G. G. Luther, C. De Angelis, A. M. Rubenchik, and S. K. Turitsyn, Phys. Rev. Lett. **75**, 73 (1995); E. W. Laedke, K. H. Spatschek, S. K. Turitsyn, and V. K. Mezentsev, Phys. Rev. E **52**, 5549 (1995).